Journal of Pharmaceutical Analysis 13 (2023) 156–169

Contents lists available at ScienceDirect

Journal of Pharmaceutical Analysis

journal homepage: www.elsevier.com/locate/jpa

Original article

Celastrol targeting Nedd4 reduces Nrf2-mediated oxidative stress in astrocytes after ischemic stroke

Zexuan Hong [a, b, 1], Jun Cao [a, 1], Dandan Liu [c, 1], Maozhu Liu [d], Mengyuan Chen [e], Fanning Zeng [a], Zaisheng Qin [a, *], Jigang Wang [c, **], Tao Tao [b, ***]

[a] Department of Anesthesiology, Nanfang Hospital, Southern Medical University, Guangzhou, 510515, China
[b] Department of Anesthesiology, Central People's Hospital of Zhanjiang, Zhanjiang, Guangdong, 524045, China
[c] Artemisinin Research Center, Institute of Chinese Materia Medica, China Academy of Chinese Medical Sciences, Beijing, 100700, China
[d] Department of Pharmacy, West China Hospital, Sichuan University, Chengdu, 610000, China
[e] Department of Pharmacy, Xi'an Daxing Hospital, Xi'an, 710000, China

ARTICLE INFO

Article history:
Received 21 June 2022
Received in revised form
13 December 2022
Accepted 30 December 2022
Available online 7 January 2023

Keywords:
Celastrol
Cerebral ischemia
Reperfusion injury
Oxidative stress
Nedd4
Nrf2
Ubiquitylation

ABSTRACT

Stroke is the second leading cause of death worldwide, and oxidative stress plays a crucial role. Celastrol exhibits strong antioxidant properties in several diseases; however, whether it can affect oxidation in cerebral ischemic-reperfusion injury (CIRI) remains unclear. This study aimed to determine whether celastrol could reduce oxidative damage during CIRI and to elucidate the underlying mechanisms. Here, we found that celastrol attenuated oxidative injury in CIRI by upregulating nuclear factor E2-related factor 2 (Nrf2). Using alkynyl-tagged celastrol and liquid chromatography-tandem mass spectrometry, we showed that celastrol directly bound to neuronally expressed developmentally downregulated 4 (Nedd4) and then released Nrf2 from Nedd4 in astrocytes. Nedd4 promoted the degradation of Nrf2 through K48-linked ubiquitination and thus contributed to astrocytic reactive oxygen species production in CIRI, which was significantly blocked by celastrol. Furthermore, by inhibiting oxidative stress and astrocyte activation, celastrol effectively rescued neurons from axon damage and apoptosis. Our study uncovered Nedd4 as a direct target of celastrol, and that celastrol exerts an antioxidative effect on astrocytes by inhibiting the interaction between Nedd4 and Nrf2 and reducing Nrf2 degradation in CIRI.

1. Introduction

Stroke, the second leading cause of mortality worldwide, is responsible for 11.6% (95% uncertainty interval 10.8%–12.2%) of total deaths and the number of deaths has been growing over the past two decades [1]. Ischemic stroke accounts for approximately 87% of all cases [2]. At present, the two main treatment strategies for acute ischemic stroke are intravenous thrombolysis and endovascular thrombectomy, which help quickly restore blood flow to the brain. During reperfusion, recanalization of blocked cerebral vessels increases glucose and oxygen levels, which can lead to cerebral ischemia-reperfusion injury (CIRI) and thus worsen the symptoms and outcomes of patients. Unfortunately, few drugs show satisfactory neuroprotective effects against CIRI, making it essential to investigate effective treatments for ischemic strokes.

Oxidative stress plays a crucial role in neuronal damage during CIRI and is characterized by excessive production of reactive oxygen species (ROS) [3,4]. Brain tissues are susceptible to oxidative damage owning to their high oxygen consumption, abundant unsaturated fatty acids, and abundant iron [5]. During ischemia and subsequent reperfusion, neuronal cells generate massive amounts of ROS, which overwhelms its elimination and disrupt the homeostasis of antioxidant systems [6]. In addition to neurons, astrocytes, microglia, and endothelial cells undergo severe oxidative stress [7,8]. ROS accumulation can trigger lipid peroxidation and damage macromolecules such as DNA and proteins [9,10]. Moreover, ROS can aggravate neuroinflammation by activating inflammatory cells and can also induce neuronal deaths by modulating apoptosis, necrosis, ferroptosis, and autophagy [3,6,11]. As one of the key players in CIRI, oxidative stress is considered as a promising target for treatment. Numerous studies have found that some antioxidant drugs, such as edaravone, allopurinol, ascorbic acid, and cajaninstilbene acid [12,13], exhibit neuroprotective effects and ameliorate neurological function after ischemic stroke.

Peer review under responsibility of Xi'an Jiaotong University.
* Corresponding author.
** Corresponding author.
*** Corresponding author.
E-mail addresses: mzkqzs@smu.edu.cn (Z. Qin), jgwang@icmm.ac.cn (J. Wang), taotaomzk@smu.edu.cn (T. Tao).
[1] These authors contributed equally to this work.

https://doi.org/10.1016/j.jpha.2022.12.002

Celastrol is a natural bioactive compound extracted from the roots of the traditional Chinese medicine *Tripterygium wilfordii* [14]. Several studies have shown that celastrol exhibits multiple biological activities, including anti-oxidative, anti-obesity, anti-inflammatory, and anti-cancerous activities [14,15]. Celastrol shows great potential for clinical applications, and two clinical trials are currently recruiting healthy volunteers to evaluate the safety of celastrol (NCT05413226 and NCT05413226) [16,17]. Celastrol can suppress oxidative stress by increasing antioxidases (superoxide dismutase (SOD) and glutathione peroxidase (GPx)), upregulating antioxidant proteins (nuclear factor E2-related factor 2 (Nrf2), silent information regulator factor 2-related enzyme 1 (SIRT1), and SIRT3), and decreasing malondialdehyde (MDA), inducible nitric oxide synthase (iNOS), and cyclooxygenase-2 (COX-2) [18–20]. By defending against oxidative damage, celastrol shows great potential in treating many neurodegenerative diseases such as Alzheimer's disease (AD), Parkinson's disease (PD), and Huntington's disease (HD) [19–21]. To date, several studies have demonstrated that celastrol enhances M2 polarization of microglia/macrophages [22] and reduces neuronal apoptosis by directly binding to high mobility group box 1 (HMGB1) [23], thus attenuating CIRI. However, few studies have explored whether celastrol can attenuate the oxidative stress induced by CIRI or target other cell types in the central nervous system (CNS).

In this study, we first tested the hypothesis that celastrol protects against oxidative stress caused by CIRI via canonical transient middle cerebral artery occlusion (tMCAO) and oxygen-glucose deprivation/reoxygenation (OGD/R) models in vivo and in vitro, respectively. Subsequently, celastrol-probed and probe-based chemical proteomics were adopted to undermine the potential target molecules and mechanisms. Our data showed that celastrol directly bound neuronally expressed developmentally down-regulated 4 (Nedd4) to regulate the ubiquitylation of Nrf2 in astrocytes, which ultimately attenuated oxidative stress to yield neuroprotection. In summary, our study reveals that Nedd4 is a target of celastrol, which may be a promising candidate for the treatment of CIRI.

2. Materials and methods

2.1. Animals

Male C57BL/6 J mice (22 ± 2 g, 8–10 weeks old) were procured from the Central Animal Facility of Southern Medical University (Guangzhou, China). The animals were housed under a pathogen-free conditions with a 12 h light/dark cycle, controlled temperature, and suitable humidity, and given free access to food and water. All experiments were performed in accordance with the National Institutes of Health Guidelines for the Care and Use of Laboratory Animals and the Institutional Animal Ethical Care Committee of Southern Medical University Experimental Animal Centre.

2.2. tMCAO model and drug treatment

The tMCAO model was performed as previously reported [24]. Briefly, the mice were anesthetized with sevoflurane (3% induction and 1.5% maintenance). After exposing and isolating the right common, external, and internal carotid arteries, the superior thyroid and occipital arteries were cauterized to reduce bleeding. A monofilament (~2 cm) was delivered to the middle cerebral artery. After 1.5 h, reperfusion was allowed by carefully removing the monofilaments. Similar surgical procedures were followed on the sham group without middle cerebral artery occlusion. Mice subjected to tMCAO were randomly divided into the following groups: tMCAO + vehicle, tMCAO + celastrol (tMCAO + cel), and tMCAO + celastrol + brusatol (tMCAO + cel + bru). Celastrol (4.5 mg/kg, Selleck Co., Ltd., Shanghai, China) and/or brusatol (0.25 mg/kg, Selleck Co., Ltd.) were administered intraperitoneally at the onset of reperfusion. The sham and tMCAO + vehicle groups were injected with an equal volume of physiological saline.

2.3. Infarct volume measurement

The 2,3,5-triphenyltetrazolium chloride (TTC) staining was conducted to analyze the cerebral infarct volume 1 day after tMCAO. After the mice were anesthetized, their brains were removed quickly and sectioned into 2-mm tissue slices. The fresh slices were stained with 2% TTC (Sigma-Aldrich, St. Louis, MO, USA) at 37 °C for 20 min and soaked in 4% formaldehyde for 24 h. The infarcted area is presented as the area of the non-ischemic hemisphere minus the non-infarcted area of the ischemic hemisphere. The infarct area was traced and analyzed using ImageJ 1.52a. The percentage of cerebral infarction was calculated using the following formula: percentage (%) of cerebral infarction = volume of the infarcted area/volume of the non-ischemic hemisphere × 100%. The interventions for each group (n = 7) are described in detail in Section 2.2.

2.4. Neurological scoring

The neurological deficit (ND) score was assessed by a blinded investigator 24 h after reperfusion as previously described [25]. The scoring system was as follows: 1) no neurological deficit (0 point), 2) forelimb weakness and torso turning to the ipsilateral side when held by the tail (1 point), 3) circling to the affected side (2 points), 4) inability to bear weight on the affected side (3 points), and 5) no spontaneous locomotor activity or barrel rolling (4 points). The interventions for each group (n = 7) are described in detail in Section 2.2.

2.5. Rotarod test

Before tMCAO, the mice were trained for 2 days (10 trials per day). After 24 h of reperfusion, the mice were placed on a suspended rod, which was accelerated from 4 to 40 rpm within 5 min. The trial ended when the mice fell off the rotarod or after reaching 300 s. Each mouse underwent three trials with a resting time of 5 min between each trial. The mean latency was used for further calculations. The interventions for each group (n = 7) are described in detail in Section 2.2.

2.6. Primary astrocytes culture

Cultured astrocytes were extracted from the brains of postnatal (P1 to P3) C57BL/6 J mice. Briefly, the cortices were collected quickly and the vascular membranes were removed. Then, the tissues were digested with 0.25% trypsin-ethylenediamine tetraacetic acid and deoxyribonuclease I (Roche Diagnostics GmbH Co., Ltd., Mannheim, Germany) for 10 min at 37 °C and filtered through a cell strainer. After centrifugation, cells were resuspended and cultured in a humidified incubator. The culture medium was replaced every two days.

2.7. Primary neuron culture

Cortical neurons were harvested from the cortices of the C57BL/6 J mouse embryos (E16-18). Cortices were mechanically dissociated into single cells. After passing through a 40-μm mesh filter, the cells were resuspended in Neurobasal Medium (Invitrogen/Life Technologies, Carlsbad, CA, USA) containing B27 (Invitrogen/Life

Technologies) and GlutaMAX (Invitrogen/Life Technologies) and plated on poly-L-ornithine and laminin (PLL)-coated plates (Sigma-Aldrich). Half of the neuron medium was replaced with fresh medium every three days.

2.8. Neuron-astrocyte co-culture

The neuron-astrocyte co-culture method was modified according to a previously described protocol [26]. Briefly, neurons were seeded in PLL-coated 6-well plates. Astrocytes were seeded on 0.4-μm Transwell inserts (Corning Inc., Corning, NY, USA). Before OGD/R, the Transwell was placed above the neurons, and both media were replaced with glucose-free Dulbecco's modified Eagle's medium (DMEM).

2.9. Human embryonic kidney (HEK) 293 T cell cultures

HEK 293 T cells were cultured in DMEM supplemented with 10% fetal bovine serum. Cells were passaged every two days. Prior to the experiments, the cells were tested negative for mycoplasma contamination.

2.10. Cell transfection

Cells were transfected with plasmids or siRNA using Lipofectamine 3000 (Invitrogen/Life Technologies) reagent following the manufacture's guidelines. After adding the transfection reagent for 6 h, the medium was discarded and replaced with a fresh medium. Further experiments were conducted 48 h after transfection.

2.11. OGD/R model

For neurons, the original medium was collected and saved, the cultured neurons were washed with Phosphate buffered saline (PBS), and glucose-free DMEM was added. The neurons were then transferred to an incubator and continuously gassed with 94% N_2, 5% CO_2, and 1% O_2 for 4 h. The medium was then replaced with Neurobasal Medium. Control cells were maintained in Neurobasal medium.

For astrocytes, the medium was replaced with glucose-free DMEM, and the cells were placed in a hypoxic chamber for 5 h.

Celastrol was dissolved in dimethyl sulfoxide (DMSO) and diluted to the indicated concentrations in the culture medium. After celastrol treatment for 1 h, the medium was replaced with a fresh medium. Culture medium with 0.01% DMSO was used in the control group. The cells were harvested 24 h after reoxygenation.

2.12. Cell viability

Primary cortical neurons were cultured on the plates. After OGD/R and drug treatment, 0.5 mg/mL 3-[4,5-dimethylthiazol-2-yl]-2,5-diphenyltetrazolium bromide solution was added and incubated for 2 h at 37 °C. Then, the supernatants were discarded, DMSO was added, and the absorbance was measured at 495 nm.

2.13. Determination of oxidative stress

To measure ROS production, either the ischemic cortex or cultured cells were prepared as single cells. The cells were incubated with 2',7'-dichlorodihydrofluorescein diacetate (Jiancheng Bioengineering, Nanjing, China) at 37 °C for 30 min, and then the fluorescence intensity (λ_{ex} = 488 nm, λ_{em} = 525 nm) was measured. The activity of SOD, GPx, catalase (CAT), and the level of MDA were measured using kits purchased from Beyotime Biotech Inc. (Shanghai, China). For the ischemic cortex test, each group consisted of three to six mice. All procedures were performed according to the manufacturer's instructions.

2.14. Terminal deoxynucleotidyl transferase dUTP nick-end labeling (TUNEL) assay

Neuron apoptosis was detected by TUNEL staining following the instructions of the kit purchased from Vazyme Biotech Co., Ltd. (Nanjing, China). Cells were fixed and permeabilized, after which cells were added to a mixture containing fluorescein isothiocyanate-12-dUTP at 37 °C for 1 h. After washing three times, the cells were incubated with mounting medium containing 4',6-diamidino-2-phenylindole (DAPI; Solarbio Science & Technology Co., Ltd., Beijing, China).

2.15. RNA extraction and real-time quantitative polymerase chain reaction (RT-PCR)

Total RNA in the cells or cerebral cortex of the mice was extracted using RNAiso purchased from Takara Bio Inc. (Shiga, Japan) following the manufacturer's protocol. After reverse transcription, RT-PCR was performed using an ABI 7500 system (Applied Biosystems, Waltham, MA, USA). Quantitative analysis was performed using the $2^{-\Delta\Delta Ct}$ method after normalizing to the mRNA level of β-actin. The primers used are listed in Table S1.

2.16. Western blotting

The penumbra area and cultured cells were lysed, and protein samples were separated by 6%–12% sodium dodecyl sulfate (SDS)-polyacrylamide gel electrophoresis and subsequently transferred onto polyvinylidene fluoride membranes (Millipore, Bedford, MA, USA). The membranes were then incubated overnight at 4 °C with corresponding primary antibodies. Membranes were blocked for 1 h and then incubated with secondary antibodies. Immunoreactive bands were detected with enhanced chemiluminescence (ECL) reagents. The primary antibodies used are listed in Table S2.

2.17. Pull down/liquid chromatography-tandem mass spectrometry (LC-MS/MS)

Pull-down/LC-MS/MS was performed to identify the targets of celastrol in astrocytes according to a previous description [23]. Astrocytes were treated with celastrol probe (cel-p) (4 μM) with or without a competitor (celastrol, 8×), for 2 h. After collecting the protein lysate of cells, click chemistry reaction was conducted with biotin azide (50 μM), sodium ascorbate (NaVc) (1 mM), tris(3-hydroxypropyltriazolylmethyl)amine (THPTA) (100 μM), and $CuSO_4$ (1 mM), which were purchased from Sigma-Aldrich (Sigma-Aldrich Co., Ltd.). Then, pre-cooled acetone was added to precipitate the proteins, which were re-dissolved in 0.1% SDS. Washed agarose beads were then added to pull down the proteins. Subsequently, the proteins were digested and isolated from the beads, followed by spin drying. The samples were labeled with distinct TMT10 isobaric peptide tags, desalted, and submitted for LC-MS/MS analysis (Thermo Fisher Scientific Inc., Boston, MA, USA).

2.18. Cellular thermal shift assay (CETSA)

Primary astrocytes were harvested using PBS containing protease inhibitors and lysed by freezing and thawing cycles in liquid nitrogen and repeated mechanical crushing. After centrifugation to collect the lysate supernatant, proteins (1 mg) from different groups were treated with either DMSO or celastrol (20 μM) for 1 h

with gentle shaking at room temperature. Then, the supernatant was divided into eight parts and heated to the designated temperatures. After cooling, the samples were centrifuged to collect the supernatant, and Western blotting was performed.

2.19. Immunoprecipitation

For ubiquitination assays, MG132 (10 μM, Selleck Co., Ltd., Shanghai, China) was added to the cells for 4 h prior to lysate collection. Then, the cells were lysed and centrifuged, after which the supernatant was incubated with anti-Nrf2 overnight at 4 °C. Protein A/G beads obtained from Beyotime Biotech Inc. were added to collect the immunocomplexes. The beads were then washed with radioimmunoprecipitation assay lysis buffer and boiled with sample buffer for Western blot analysis.

2.20. Immunofluorescence staining

At 24 h after tMCAO, the mice were deeply anesthetized and perfused intracardially with saline and 4% paraformaldehyde from Solarbio Science & Technology Co., Ltd.. After fixation, brains were dehydrated and cut into frozen coronal slices (20 μm). The brain slices were fixed, permeabilized, and blocked. Then, the slices were incubated overnight at 4 °C with the primary antibodies (1:250). Thereafter, the brain slices were washed and incubated with fluorescently labeled secondary antibodies (1:500). DAPI was obtained from Solarbio Science & Technology Co., Ltd. and was used for counterstaining. Fluorescent staining was performed using a laser scanning confocal microscope (LSM900, Carl Zeiss IMT Co., Ltd., Oberkochen, Germany).

To detect the colocalization of cel-p and Nedd4, cultured cells were treated with cel-p. After washing with PBS, the cells were fixed and permeabilized. The cells were subsequently incubated with click chemistry reaction reagents containing NaVc (1 mM), THPTA (100 μM), $CuSO_4$ (1 mM), and tetramethylrhodamine-phenyl azide (50 μM) for 2 h at room temperature. The cells were then washed and blocked with 3% bovine serum albumin. Immunofluorescence staining was performed as described above.

2.21. Statistical analysis

Statistical analyses were performed using GraphPad Prism 7. Differences between the two groups were evaluated using the Student's t-test. For analysis of more than two groups, differences were evaluated by one-way analysis of variance (ANOVA) when the sample amounts were consistent or by two-way ANOVA (Bonferroni's multiple comparisons test) when the sample amounts were inconsistent between different groups. $P < 0.05$ was considered statistically significant ($^{*}P < 0.05$, $^{**}P < 0.01$, $^{***}P < 0.001$, and $^{****}P < 0.0001$).

3. Results

3.1. Celastrol reduced cerebral infarction and improved neurological functional outcome

We first confirmed the neuroprotection of celastrol (Fig. 1A) on mice after tMCAO. The experimental scheme of this study is presented in Fig. 1B. TTC staining was used to evaluate infarct size in the mice. As shown in Figs. 1C and D, after tMCAO, celastrol significantly decreased the infarct volumes compared to the vehicle-treated tMCAO group.

More severe neuronal damage was observed in the model group compared to the sham group, and such morphological lesions were markedly attenuated in the celastrol-treated group (Figs. 1E and F). Accordingly, CIRI increased neuronal apoptosis, while celastrol obviously downregulated apoptosis in the ischemic cerebral cortex than in the model group (Figs. 1E and G).

To assess the effects of celastrol on neurological function, we performed neurological scoring and rotarod test 24 h after focal ischemia/reperfusion (I/R). Mice treated with celastrol showed a reduction in ND score (Fig. 1H) and a significant improvement in motor function (Fig. 1I). These data indicated that celastrol protected the brain from I/R injury and enhanced neurological function after stroke.

3.2. Celastrol attenuated oxidative stress after CIRI

Oxidative stress plays an important role in cerebral I/R injury. To investigate whether celastrol could attenuate oxidative injury after tMCAO, we assessed oxidative damage. As shown in Fig. 2A, ROS production was notably higher in the tMCAO group than in the sham group. Celastrol administration significantly decreased ROS production compared to that in the model group. Moreover, iNOS was upregulated in the tMCAO group, whereas celastrol clearly downregulated iNOS expression (Fig. 2B).

Meanwhile, the activities of SOD, CAT, and GPx were remarkably inhibited and the MDA content increased in the tMCAO group compared to the sham group. However, celastrol significantly recovered the activities of SOD, CAT, and GPx and reduced MDA levels relative to the model group (Figs. 2C–F).

Additionally, celastrol affected the transcription of genes related to oxidative stress (Fig. 2G). We further validated the translation of these genes by Western blotting, and protein levels were corresponding to the mRNA levels (Figs. 2H and I). These results suggested that celastrol attenuated oxidative stress after CIRI.

3.3. Celastrol alleviated oxidative damage via upregulating Nrf2

To investigate the anti-oxidative mechanism of celastrol, we analyzed the transcription profile based on RNA-Seq data of the ischemic hemisphere of celastrol-treated mice versus vehicle-treated mice (GSE202659). The analysis showed that 168 genes were upregulated while 156 were downregulated in celastrol-treated mice (Fig. 3A). Subsequently, we conducted Gene Ontology (GO) enrichment analysis for these differentially expressed genes (DEGs). GO analysis revealed that DEGs were involved in several terms such as oxidoreductase activity, homeostatic process, and mitochondria, which were closely related to oxidative stress (Fig. 3B). The protein-protein interaction network of these DEGs showed that Nrf2 had multiple connections with the DEGs and that celastrol could upregulate the level of Nrf2 after CIRI (Figs. 3C and D). Thus, Nrf2 might be attributed to the antioxidant effects of celastrol after CIRI.

To further confirm that celastrol attenuated oxidative stress by modulating Nrf2, brusatol, a unique inhibitor of Nrf2, was used to decrease the level of Nrf2. After tMCAO, mice were treated with celastrol and brusatol. We found that both infarction volume and morphological lesions, which were attenuated by celastrol after CIRI, were aggravated by brusatol (Figs. 3E, F, and S1). Moreover, Nrf2 inhibition abrogated the effects of celastrol on the ND score (Fig. 3G) and motor function (Fig. 3H) after CIRI.

Next, we investigated the level of oxidative stress in vivo after blocking Nrf2. As shown in Fig. 3I, the reduction in ROS by celastrol was terminated by brusatol. We also found that brusatol upregulated iNOS levels, even after treatment with celastrol (Figs. 3J and K). Additionally, brusatol blocked the increase in SOD, CAT, and GPx activities and the decrease in MDA content, which were caused by celastrol (Fig. 3L). These results suggested that Nrf2 was required for the antioxidant activity of celastrol in CIRI.

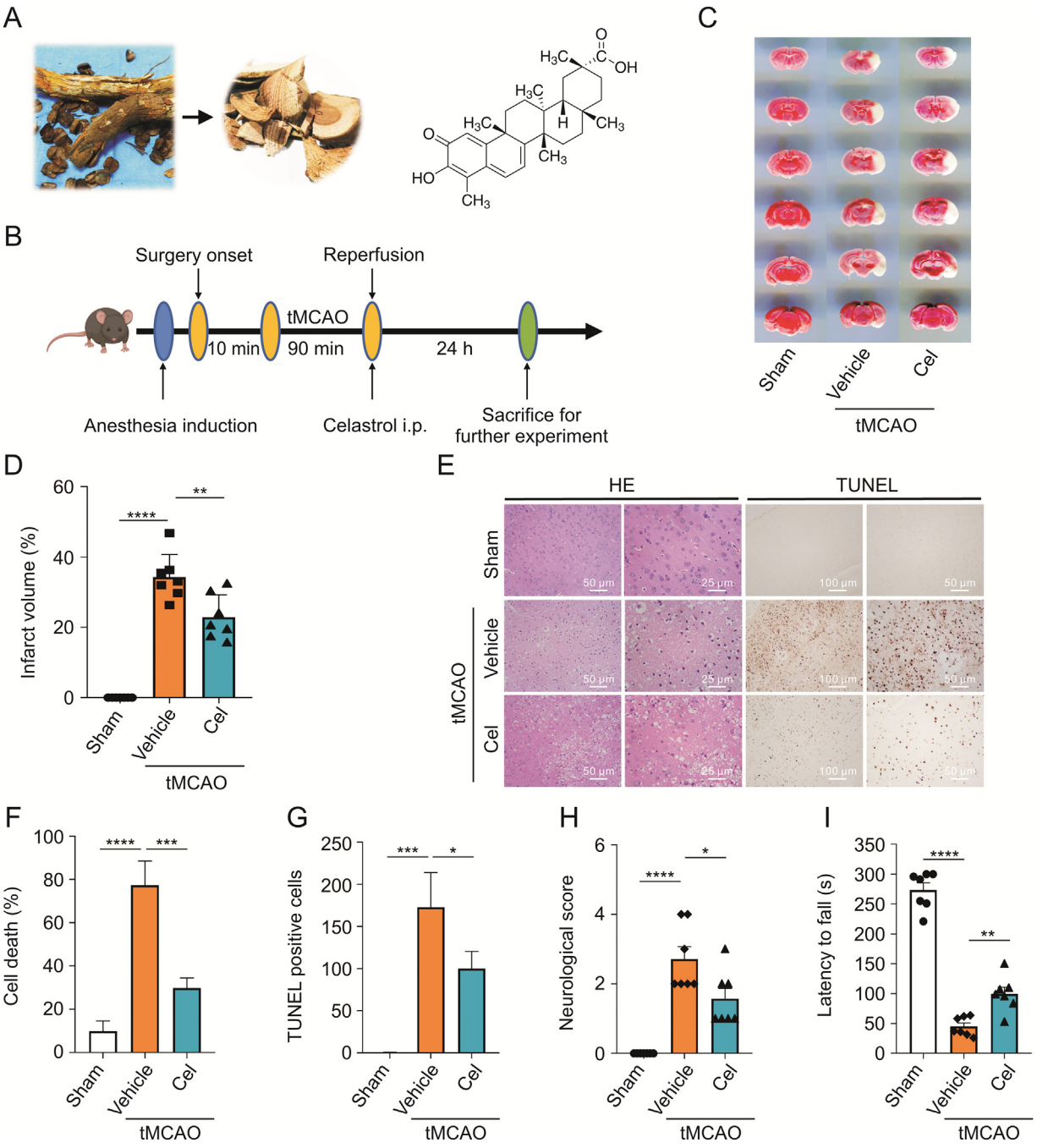

Fig. 1. Celastrol significantly reduced cerebral infarction area in transient middle cerebral artery occlusion (tMCAO) mice. (A) Source and chemical structure of celastrol. (B) Overall scheme of the experiment design. (C and D) TTC staining of the brain slices and the percentage of the infarct volume. (E) hematoxylin and eosin (HE) and terminal deoxynucleotidyl transferase dUTP nick-end labeling (TUNEL) staining of brain sections. (F) Percentage of dead cells in the ischemic hemisphere. (G) Quantification of TUNEL-positive cells in the ischemic hemisphere. (H) Neurological deficit score of the mice. (I) Assessment of motor function by rotarod test. i.p.: intraperitoneal injection; cel: celastrol. All data shown are the means ± standard error of the mean ($n = 7$). $^{*}P < 0.05$, $^{**}P < 0.01$, $^{***}P < 0.001$, and $^{****}P < 0.0001$.

3.4. Celastrol reduced the oxidative stress by decreasing the ubiquitylation of Nrf2 in astrocytes

To explore whether celastrol directly reduces oxidative stress in neurons, we applied celastrol to primary cultured neurons after OGD/R. Inconsistent with our hypothesis, we found that celastrol had little effect on neuronal ROS after OGD/R, even when we increased the concentration and duration of celastrol (Figs. S2A–C). Thus, it is likely that the direct target cells of celastrol's antioxidant activity were other types of cells in the brain.

Astrocytes, the most abundant cells in the mammalian brain, perform a variety of functions in the CNS [27,28]. We investigated whether celastrol attenuates oxidative stress after CIRI by targeting astrocytes. Primary astrocytes were treated with celastrol (1.5 μM) for 1 h immediately after OGD. As shown in Fig. 4A, celastrol significantly reduced ROS production in primary cultured astrocytes after OGD/R. Moreover, increased Nrf2 expression was observed in astrocytes instead of neurons after celastrol treatment in tMCAO mice (Fig. S3A). HO-1 also showed the same tendency as Nrf2 in astrocytes (Fig. S3B). Consistent with the in vivo results,

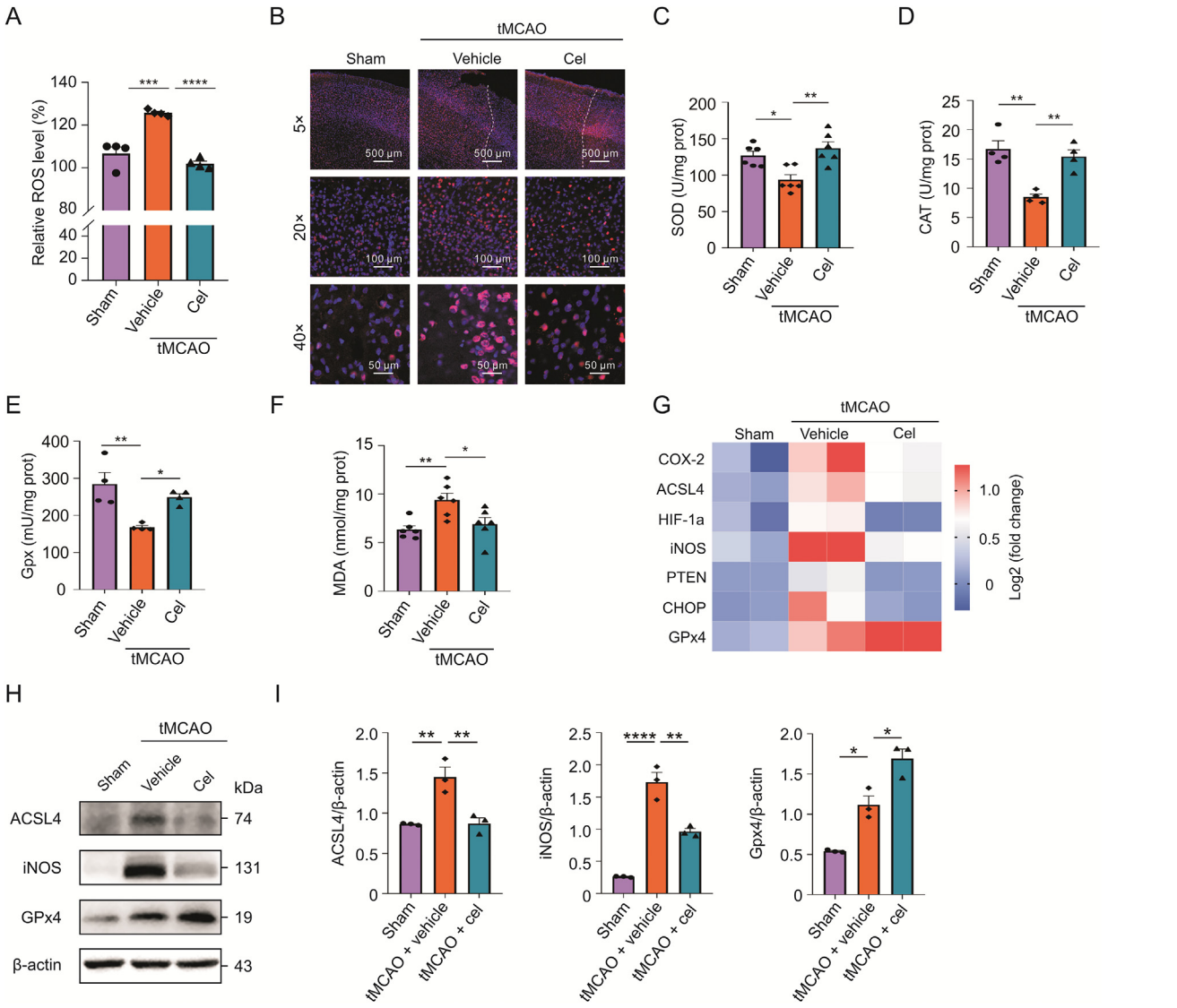

Fig. 2. Celastrol attenuated the oxidative stress after cerebral ischemic-reperfusion injury (CIRI). (A) Level of reactive oxygen species (ROS) in the brain tissues. (B) Immunostaining of inducible nitric oxide synthase (iNOS) in penumbra area. (C–F) Assessment of superoxide dismutase (SOD), catalase (CAT), glutathione peroxidase (GPx), and malondialdehyde (MDA) in brain tissues. (G) Heatmap presenting differentially expressed genes (DEGs) related to oxidative stress in different groups: each group involved two biological replicates containing three mice. (H and I) Protein expression of ACSL4, iNOS, and GPx4 in different groups measured by Western blotting analysis. All data shown are the means ± standard error of the mean ($n = 3–6$). cel: celastrol; tMCAO: transient middle cerebral artery occlusion; HIF-1α: hypoxia-inducible factor-1alpha; PTEN: phosphatase and tensin homolog; CHOP: CCAAT/enhancer-binding protein homologous protein. $^{*}P < 0.05$, $^{**}P < 0.01$, $^{***}P < 0.001$, and $^{****}P < 0.0001$.

Nrf2, HO-1, and GPx4 were upregulated and iNOS was down-regulated in astrocytes OGD/R treated with celastrol (Figs. 4B–D). Glial fibrillary acid protein staining revealed that astrocytes were strikingly activated after OGD/R, and celastrol administration inhibited astrocyte transformation (Fig. 4E).

To further explore the mechanism by which celastrol regulates Nrf2 in astrocytes, we assessed the mRNA level of Nrf2 and found that celastrol did not affect the transcription of Nrf2 (Fig. 4F).

Multiple studies have concluded that Nrf2 is modulated in a post-translational manner, and ubiquitin-dependent degradation is an important mechanism in the regulation of Nrf2 [29]. Thus, we investigated the ubiquitination of Nrf2 at different time points after reoxygenation. In the ubiquitination assays, Nrf2 was ubiquitinated 6, 12, and 24 h after OGD/R (Figs. 4G and S4). However, celastrol applied to astrocytes significantly suppressed the ubiquitinoylation of Nrf2 24 h after OGD/R (Fig. 4G). Taken together, these results demonstrated that celastrol reduced oxidative stress and attenuated the reaction of astrocytes by increasing Nrf2.

3.5. Inhibiting Nrf2 weakened the antioxidant effect of celastrol in astrocytes

To further confirm that Nrf2 contributes to celastrol's antioxidant activity in astrocytes, we treated astrocytes with both celastrol and brusatol. We found that inhibiting Nrf2 significantly increased ROS production, even in the presence of celastrol (Fig. 5A). The effects of celastrol on the translation of Nrf2, HO-1, and GPx4 were abolished by brusatol (Figs. 5B and C). Furthermore, brusatol prevented iNOS decreasing resulted from celastrol in astrocytes after OGD/R (Fig. 5D). Next, we investigated astrocyte activation by blocking Nrf2. As presented in Fig. 5E, brusatol promoted the activation of astrocytes regardless of celastrol treatment after OGD/R.

According to these results, celastrol reduced oxidative stress level in astrocytes. In vivo experiments showed that celastrol significantly improved motor ability, which was dominated by neurons. We speculated that celastrol might target astrocytes and protect neurons.

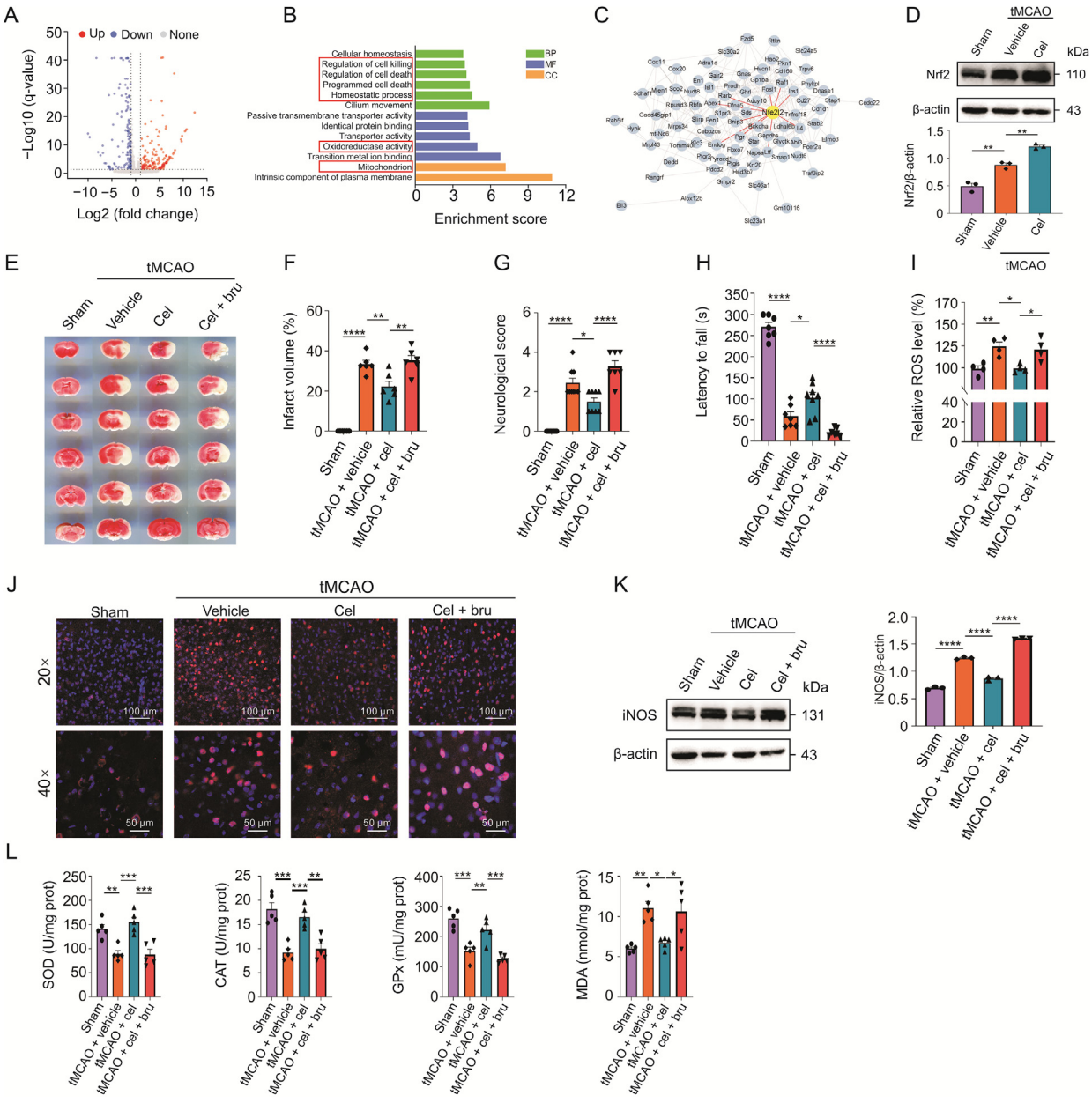

Fig. 3. Celastrol alleviates oxidative damage via upregulating nuclear factor E2-related factor 2 (Nrf2). (A) Volcano plot analysis of the differentially expressed genes (DEGs) between celastrol-treated versus vehicle-treated mice after transient middle cerebral artery occlusion (tMCAO). Upregulated, downregulated, and non-differentially expressed genes are presented in red, blue, and gray dots, respectively. (B) Gene Ontology (GO) enrichment analysis of DEGs. BP: biological process; MF: molecular function; CC: cellular component. (C) Protein-protein interaction network among the DEGs. Nrf2 (gene name: *Nfe2l2*) is highlighted. (D) Immunoblotting showed protein expression of Nrf2 in vivo. (E and F) The 2,3,5-triphenyltetrazolium chloride (TTC) staining of the brain slices and the percentage of the infarct volume ($n = 6$). (G) Neurological scores of the mice ($n = 7–9$). (H) Assessment of motor function by the rotarod test ($n = 7–9$). (I) Effect of brusatol on the production of reactive oxygen species (ROS) after cerebral ischemic-reperfusion injury (CIRI). (J) Immunostaining showing the change of inducible nitric oxide synthase (iNOS) in penumbra area after inhibiting Nrf2. (K) Immunoblotting showing the protein level of iNOS in vivo. (L) Assessment of superoxide dismutase (SOD), catalase (CAT), glutathione peroxidase (GPx), and malondialdehyde (MDA) in brusatol-treated mice after CIRI, each group consisted of four to five mice. All data shown are the means ± standard error of the mean. cel: celastrol; bru: brusatol. $^{*}P < 0.05$, $^{**}P < 0.01$, $^{***}P < 0.001$, and $^{****}P < 0.0001$.

We adopted an astrocyte-neuron coculture system, and astrocytes were treated with celastrol after OGD/R. We then assessed the damage to the cocultured neurons. TUNEL staining showed that after OGD/R, a large number of neurons underwent apoptosis, whereas celastrol effectively rescued neurons from death (Fig. 5F). In addition, celastrol remarkably attenuated OGD/R-induced axonal damage in neurons (Fig. 5G). Moreover, inhibition of Nrf2 in astrocytes diminished the neuroprotective effect of celastrol (Figs. 5F and G).

Collectively, these data indicated that Nrf2 knockdown blocked the antioxidant activity of celastrol in vitro and that celastrol directly targeted astrocytes and ultimately protected neurons after OGD/R.

3.6. Celastrol bound to Nedd4 and inhibited the ubiquitination of Nrf2 in astrocytes

Nrf2 plays critical roles in the defense against oxidative stress in the brain, particularly in CIRI [30]. To further explore the regulation of Nrf2 by celastrol, we used a cel-p, in which an alkynyl handle was linked to the carboxyl terminus of celastrol (Fig. 6A). Cel-p is capable of pulling down the directly interacting targets of celastrol

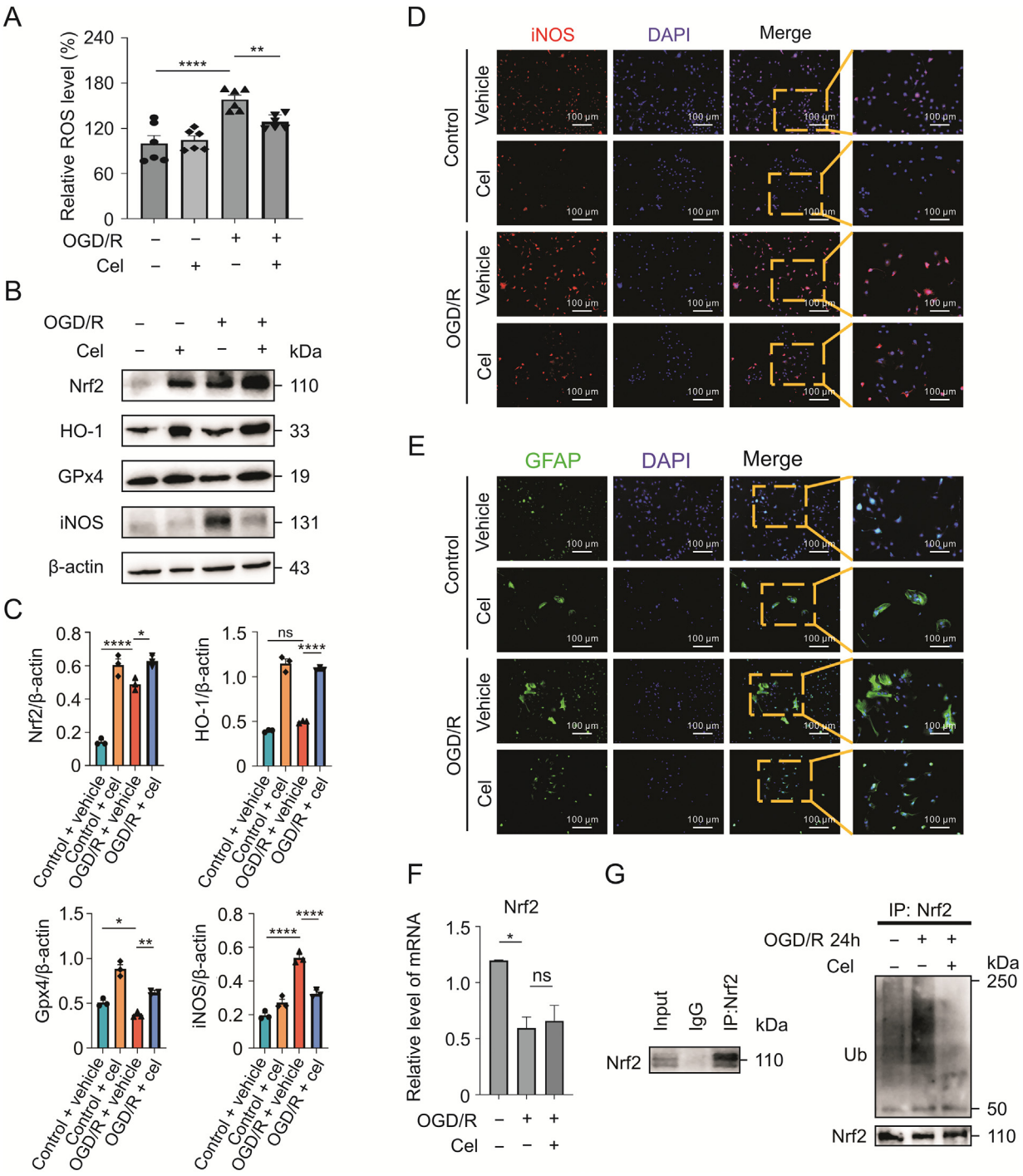

Fig. 4. Celasrol reduces the oxidative stress by decreasing the ubiquitylation of nuclear factor E2-related factor 2 (Nrf2) in astrocytes. (A) Effects of celastrol on reactive oxygen species (ROS) levels in astrocytes after oxygen-glucose deprivation/reoxygenation (OGD/R). (B and C) Protein levels of Nrf2, HO-1, glutathione peroxidase 4 (GPx4), and inducible nitric oxide synthase (iNOS) after celastrol treatment. (D) Immunostaining showing iNOS expression in astrocytes. (E) Activation of astrocytes after OGD/R following celastrol treatment. (F) The mRNA level of Nrf2 in astrocytes treated with celastrol. (G) Ubiquitinoylation of Nrf2 in astrocytes following celastrol treatment 24 h after reperfusion. Data shown are the means ± standard error of the mean. cel: celastrol; DAPI: 4',6-diamidino-2-phenylindole; GFAP: glial fibrillary acid protein. $^{*}P < 0.05$, $^{**}P < 0.01$, and $^{****}P < 0.0001$.

through click chemistry reactions. Through LC-MS/MS analysis, 1157 proteins were identified as celastrol targets (Table S3).

Surprisingly, neither Nrf2 nor kelch-like ECH-associated protein 1 (Keap1), the canonical upstream of Nrf2 [30], was included in the profiling. In addition, the binding between Nrf2 and Keap1 showed little change following celastrol treatment after OGD/R (Fig. S5A). After Kyoto Encyclopedia of Genes and Genomes analysis of the target proteins (Table S4), we screened for proteins related to ubiquitin-mediated proteolysis and noticed that Nedd4, an E3 ligase, was a reliable target of celastrol (Table S5). Furthermore, Nedd4 was predicted to be an E3 ligase for Nrf2 in the UbiBrowser database (Fig. S5B). The CETSA data also showed that compared with the control group, the direct binding of celastrol and Nedd4 reduced Nedd4 protein degradation under rising temperatures (Fig. 6B). Pull-down and Western blot revealed that celastrol (8×) completely competed for the binding of cel-p to Nedd4 (Fig. S5C),

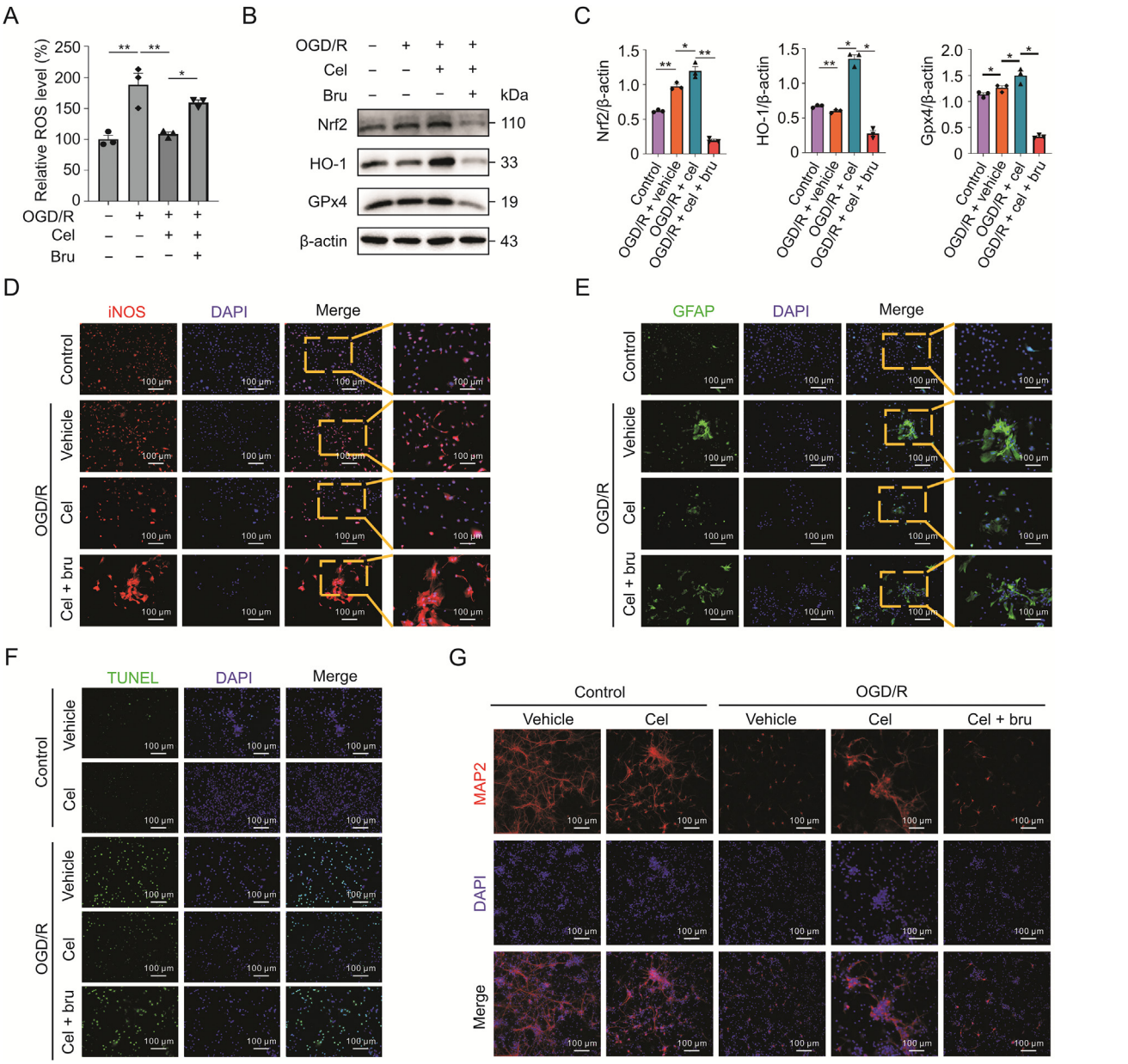

Fig. 5. Inhibiting nuclear factor E2-related factor 2 (Nrf2) weakened the antioxidant effect of celastrol in astrocytes. (A) Effect of Nrf2 inhibition on the reactive oxygen species (ROS) in astrocytes after oxygen-glucose deprivation/reoxygenation (OGD/R). (B and C) Protein levels of Nrf2, HO-1, and glutathione peroxidase 4 (GPx4) after inhibition of Nrf2. (D) Expression of inducible nitric oxide synthase (iNOS) in astrocytes after inhibition of Nrf2. (E) Activation of astrocytes after OGD/R with inhibition of Nrf2. (F) Terminal deoxynucleotidyl transferase dUTP nick-end labeling (TUNEL) assays of neurons cocultured with astrocytes treated with celastrol treatment after OGD/R. (G) Microtubule associated protein 2 (MAP2) staining reflected damage to axons. Data are shown as the means ± standard error of the mean. cel: celastrol; bru: brusatol; DAPI: 4',6-diamidino-2-phenylindole; GFAP: glial fibrillary acid protein. $^{*}P < 0.05$ and $^{**}P < 0.01$.

further verifying that Nedd4 was a direct binding target of celastrol. Thus, we hypothesized that celastrol might regulate Nrf2 by directly binding to Nedd4.

Next, we investigated the binding between celastrol and Nedd4 using click reaction and immunofluorescence staining. As shown in Fig. 6C, cel-p clearly colocalized with Nedd4, and the co-localization was reduced by adding normal celastrol as a competitor to cel-p.

We confirmed the interaction between Nedd4 and Nrf2. After overexpression of Nedd4 in astrocytes, Nrf2 was significantly decreased in addition to the downstream oxidative molecules HO-1 and GPx4 (Figs. 6D and E). Co-immunoprecipitation (IP) suggested that Nedd4 could bind to Nrf2 and that celastrol reduced this binding (Fig. 6F). Consistently, immunofluorescence revealed that after OGD/R, the colocalization of Nedd4 with Nrf2 was increased in astrocytes, and celastrol treatment could downregulate their colocalization (Fig. 6G). Thus, our data suggested that celastrol directly bound to Nedd4 and reduced the binding between Nedd4 and Nrf2 in astrocytes.

3.7. *Knockdown Nedd4 attenuated oxidative stress by reducing the ubiquitination of Nrf2*

Next, we confirmed the effect of Nedd4 on oxidative stress by inhibiting Nedd4 in astrocytes. When Nedd4 was knocked down with siRNA, the levels of Nrf2, HO-1, and GPx4 were markedly increased in siNedd4 cells compared to the controls (Figs. 7A and B). To further validate the regulation of Nedd4 on Nrf2, we evaluated the ubiquitinoylation of Nrf2 and found that knockdown of Nedd4

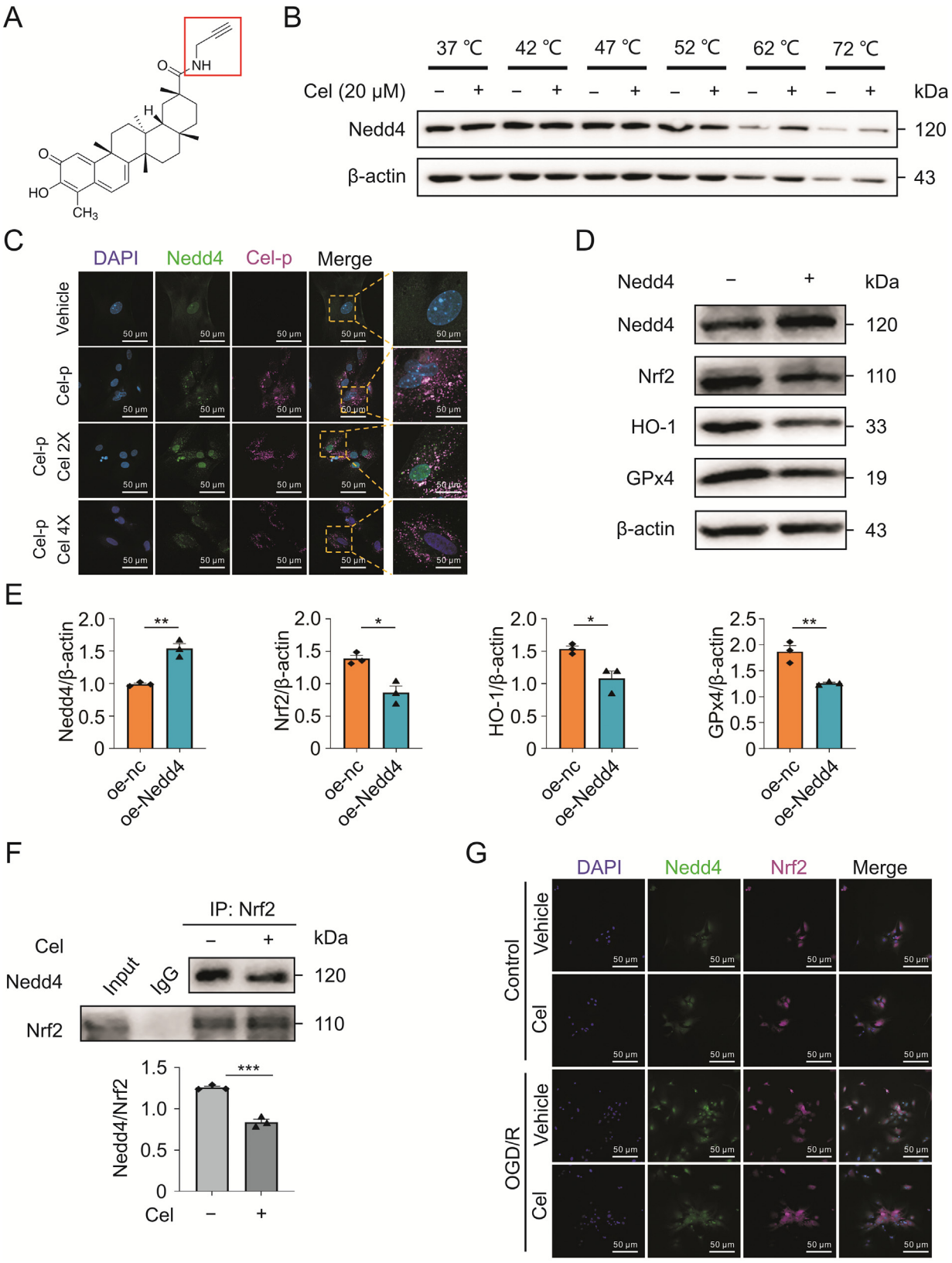

Fig. 6. Celastrol bound to neuronally expressed developmentally downregulated 4 (Nedd4) and inhibited the ubiquitination of nuclear factor E2-related factor 2 (Nrf2) in astrocytes. (A) Structural formula of labeled celastrol. (B) Cellular thermal shift assay (CETSA) showing that celastrol bound to Nedd4 and reduced Nedd4 degradation with increasing temperatures. (C) Immunofluorescence showing the colocalization of celastrol-probe (cel-p) and Nedd4. (D and E) Western blot analysis of Nrf2, HO-1, and glutathione peroxidase 4 (GPx4) after Nedd4 overexpression (oe) in astrocytes. (F) Co-immunoprecipitation revealing the effect of celastrol on the binding between Nedd4 and Nrf2. (G) Immunofluorescence showing the binding of Nedd4 and Nrf2 in celastrol-treated astrocytes. Data shown are the means ± standard error of the mean. cel: celastrol; DAPI: 4',6-diamidino-2-phenylindole; nc: negative control. $^{*}P < 0.05$, $^{**}P < 0.01$, and $^{***}P < 0.001$.

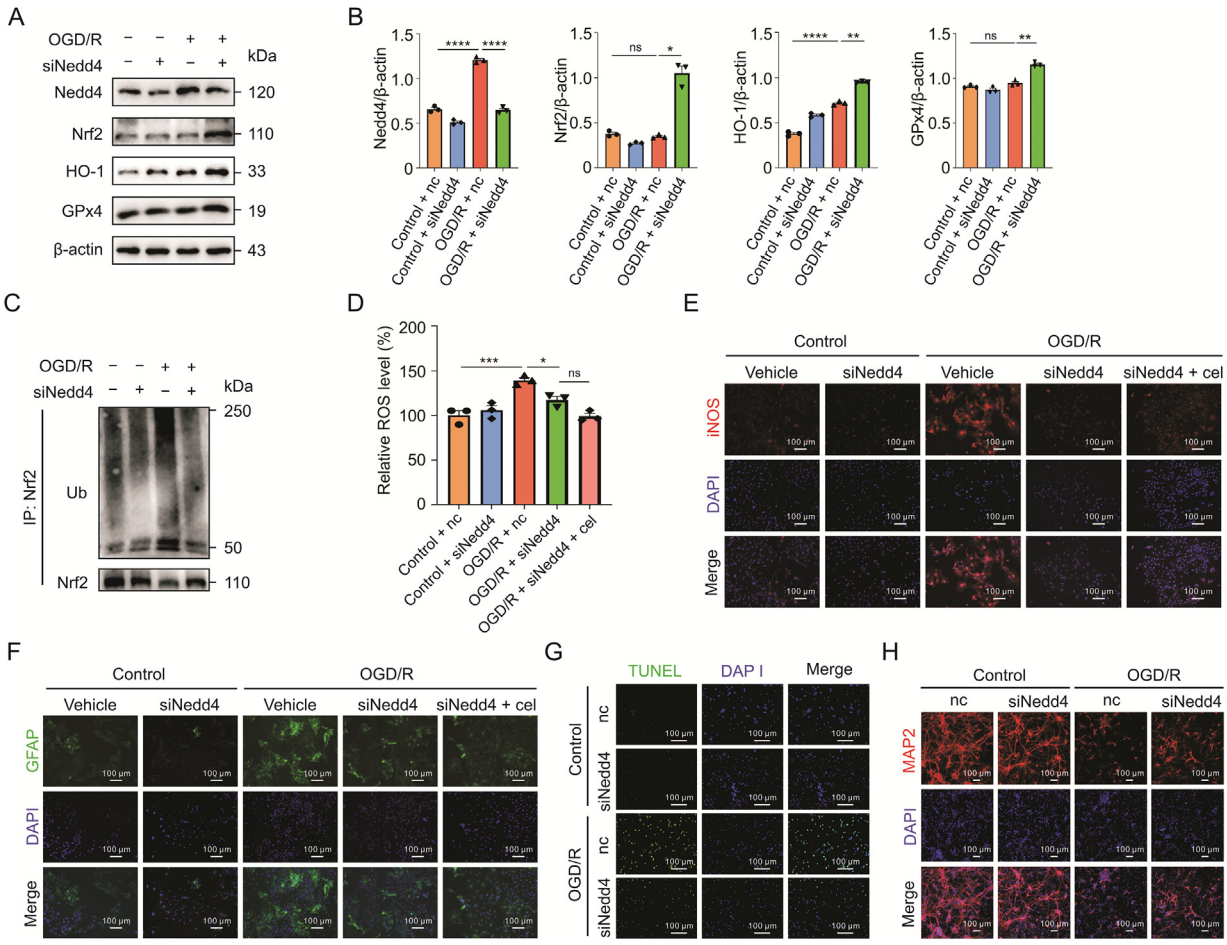

Fig. 7. Knockdown of neuronally expressed developmentally downregulated 4 (Nedd4) attenuated the oxidative stress by reducing the ubiquitinoylation of nuclear factor E2-related factor 2 (Nrf2). (A and B). Western blot analysis of the protein levels of Nrf2, HO-1, and glutathione peroxidase 4 (GPx4) after knockdown of Nedd4 (siNedd4). (C) Ubiquitinoylation of Nrf2 in astrocytes after knockdown of Nedd4 by transfecting siRNA. (D) Effect of inhibiting Nedd4 on the reactive oxygen species (ROS) of astrocytes after oxygen-glucose deprivation/reoxygenation (OGD/R). (E) Immunostaining revealing the expression of inducible nitric oxide synthase (iNOS) in astrocytes. (F) Glial fibrillary acid protein staining showing the activation of astrocytes. (G) Terminal deoxynucleotidyl transferase dUTP nick-end labeling (TUNEL) assay of neurons cocultured with astrocytes with Nedd4 knockdown after OGD/R. (H) Microtubule associated protein 2 (MAP2) staining reflecting the axonal damage. Data shown are the means ± standard error of the mean. cel: celastrol; IP: immunoprecipitation; Ub: ubiquitin; nc: negative control; DAPI: 4',6-diamidino-2-phenylindole; GFAP: glial fibrillary acid protein. $^{*}P < 0.05$, $^{**}P < 0.01$, $^{***}P < 0.001$, and $^{****}P < 0.0001$.

led to lower ubiquitinoylation of Nrf2 after OGD/R (Fig. 7C). Additionally, inhibiting Nedd4 reduced ROS accumulation, whereas adding celastrol did not further lower the ROS level (Fig. 7D). Likewise, iNOS expression was largely suppressed by knockdown of Nedd4 with or without celastrol administration (Fig. 7E).

Moreover, the knockdown of Nedd4 also alleviated the activation of astrocytes after OGD/R, which exhibited no obvious difference when combined with celastrol treatment (Fig. 7F). Furthermore, through coculture of neurons and astrocytes, we found that knockdown of Nedd4 in astrocytes also notably reduced neuronal apoptosis (Fig. 7G) and reversed axonal damage in neurons (Fig. 7H).

Overall, these results showed that Nedd4, as a direct target of celastrol, played a critical role in modulating oxidative stress in astrocytes by regulating the ubiquitination-mediated degradation of Nrf2, which ultimately affected the damage to neurons with OGD/R.

3.8. Nedd4 catalyzed K48-linked ubiquitination of Nrf2

To demonstrate the specific modulation of Nedd4 on Nrf2, we co-transfected Nedd4 and Nrf2 into HEK 293 T cells after confirming the efficiency of Nedd4 and Nrf2 plasmids (Fig. 8A). As shown in Fig. 8B, Nedd4 decreased Nrf2 protein levels in a dose-dependent manner.

To further determine the type of Nrf2 ubiquitination, we co-transfected Nrf2 with Nedd4, ubiquitin, K48-ubiquitin, and K63-ubiquitin into HEK 293 T cells. The results showed that Nedd4 mediated K48-linked, instead of K63-linked, polyubiquitination of Nrf2 (Fig. 8C). Furthermore, celastrol significantly inhibited the K48-linked polyubiquitination of Nrf2 (Fig. 8D). C8-D1A, an immortalized astrocyte line, was also used to confirm Nedd4-catalyzed ubiquitination of Nrf2. As shown in Fig. 8E, overexpression of Nedd4 increased the K48-linked polyubiquitination of Nrf2, which was weakened by celastrol. Collectively, these results indicated that Nedd4 catalyzed K48-linked ubiquitination of Nrf2, which could be inhibited by celastrol.

4. Discussion

In the present study, we presented an updated understanding of celastrol's effect in the CIRI. We found that celastrol decreased ROS levels by upregulating Nrf2 in astrocytes, eventually reducing neuronal damage. The underlying mechanism was that celastrol

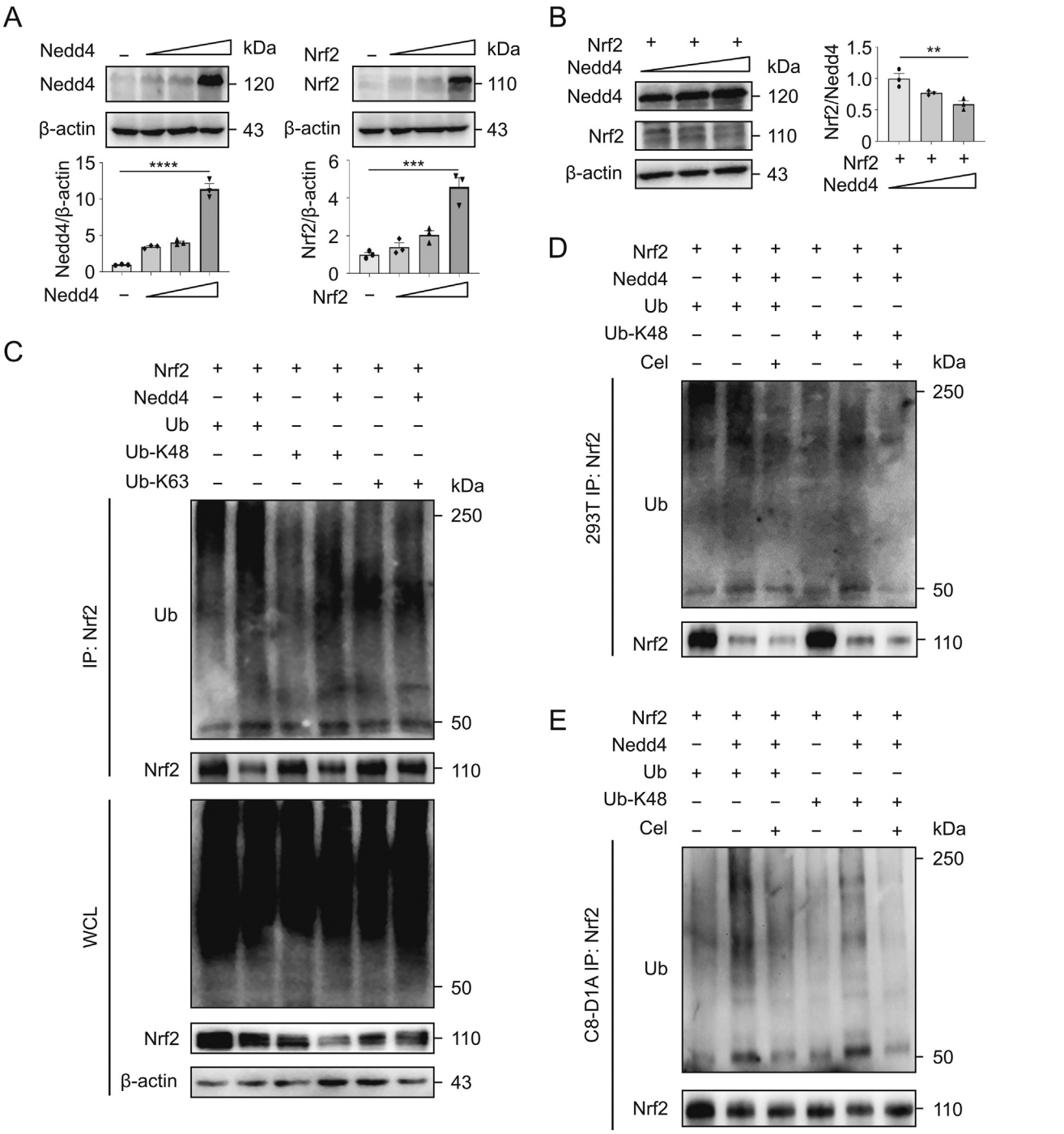

Fig. 8. Neuronally expressed developmentally downregulated 4 (Nedd4) catalyzed K48-linked ubiquitination of nuclear factor E2-related factor 2 (Nrf2). (A) Immunoblotting (IB) analysis of Nedd4 and Nrf2 respectively in human embryonic kidney (HEK) 293 T cells transfected with indicated DNA constructs (1, 3, and 5 μg). (B) Expression of Nrf2 in HEK 293 T cells co-transfected with Nrf2 (3 μg) and Nedd4 (1, 2, and 4 μg). (C) IB analysis of the level of Nrf2 in total protein and the ubiquitination of Nrf2 in HEK 293 T cells co-transfected with plasmids expressing Nrf2, Nedd4, and wild-type Ub, Ub-K48, or Ub-K63. IB analysis of ubiquitination of Nrf2 in (D) HEK 293 T and (E) C8-D1A cells when co-transfected with plasmids expressing Nrf2, Nedd4, and wild-type Ub or Ub-K48 upon celastrol treatment. Data shown are the means ± standard error of the mean. Ub: ubiquitin; cel: celastrol; IP: immunoprecipitation; WCL: whole cell lysate. $^{**}P < 0.01$, $^{***}P < 0.001$, and $^{****}P < 0.0001$.

directly bound to Nedd4 and inhibited the binding between Nedd4 and Nrf2, thus reducing the ubiquitylation-mediated degradation of Nrf2. Based on published studies, our findings provide a novel mechanism for celastrol's antioxidant capacity in ischemic stroke and identify Nedd4 as a target of celastrol.

Tripterygium wilfordii and its extracts or bioactive compounds, such as triptolide and celastrol, exhibit a variety of regulatory functions in different cell types (e.g., neuronal cell lines, astrocytes, microglia, and T helper 17 cells) in neurodegenerative diseases through various targets such as NF-κB, iNOS, and COX-2 [31,32]. As one of the effective compounds of this herb, celastrol is listed as one of five promising traditional medicines for transforming into modern drugs [33], and also shows outstanding neuroprotective effects on CIRI. Celastrol can reach the brain 30 min after administration at 100 μg/kg [34], which explains its outstanding effects in the CNS. In our previous study, we also found that celastrol binds

HMGB1 of neurons, producing anti-inflammation [23] and regulating hypoxia-inducible factor-1alpha inhibiting glycolysis [35] to yield neuroprotection in CIRI. Another study also found that celastrol protected against cerebral ischemia-induced brain injury through promoting interleukin-33/suppression of tumorigenicity 2 mediated microglia/macrophage M2 polarization [22]. Unfortunately, few studies have focused on the effect of celastrol on astrocytes in CNS diseases, and there are hardly any reports on the anti-oxidative effect of celastrol in CIRI. Recently, Wang et al. [36] found that celastrol reduced ROS generation in hippocampal neuron-22 cells by downregulating AK005401/MAP3K12 in a global cerebral ischemia-reperfusion mouse model. However, we did not find a similar effect, which may be due to the primary cultured neurons used in our experiment. Instead, we found that celastrol suppressed oxidative stress in astrocytes. Astrocytes, the most widely distributed cells in the brain [27], were activated within minutes after ischemic stroke [37]. Our previous study showed that ROS levels were elevated during hypoxia-reperfusion and could trigger the activation of astrocytes [24]. Moreover, astrocytes have higher ROS production than neurons because of the different organization of mitochondrial respiratory chain complexes [38]. Reactive astrocytes can produce free radicals, including nitric oxide, superoxide, and iNOS, after CIRI, resulting in severe neuronal death [37]. On the basis of existing studies, it is undoubted that astrocytes play an important role in regulating oxidative stress in ischemic stroke. In our study, we revealed that celastrol influenced the transformation of reactive astrocytes by regulating Nedd4/Nrf2 and suppressing ROS generation. With multi-cell targets, celastrol shows great potential in clinical applications beyond our previous expectations.

Using a probe linked to celastrol, we identified the direct binding proteins of this compound. Notably, neither Nrf2 nor Keap1, the classic regulator of Nrf2 [30], was included as an interacting protein. Thus, we propose that there is another upstream regulating ubiquitylation of Nrf2. Based on our study, Nedd4, the founding member of the Nedd4 family of homologous to E6AP carboxyl-terminus-type E3 ubiquitin ligases [39], appears to bind to celastrol and function as an E3 ligase for Nrf2. Nedd4 is highly expressed in the early embryonic brain [40] and is involved in cell proliferation, neuronal differentiation, neurite growth, and synaptic connections [41–43]. According to Kwak et al. [44], Nedd4 could alleviate zinc-induced neuronal death by degrading insulin-like growth factor-1 receptor beta. However, it is worth noting that Lackovic et al. [45] hypothesized that Nedd4 might be a protective protein in CIRI; in that, Nedd4-family interacting protein 1, an adaptor of Nedd4, is increased after CIRI and remarkably attenuates neuronal injuries. However, this hypothesis still lacks experimental proof. Here, we discovered that Nedd4 contributed to CIRI by promoting ubiquitination-mediated degeneration of Nrf2, which was inhibited by celastrol. Moreover, studies have shown that the expression of Nedd4 is upregulated in several neurodegenerative diseases such as AD, PD, and HD [46]. Therefore, Nedd4, as a target of celastrol, not only can be applied in CIRI but can also act as a promising target for celastrol application in other neurodegenerative diseases.

Nrf2 is an important molecule in maintaining redox homeostasis in the brain, skeletal muscle, liver, lungs, and other organs [47–49]. In pathological conditions, such as excessive accumulation of ROS, Nrf2 is translocated into the nucleus, promoting the transcription of protective molecules, which defends cells against damage from oxidative stress. According to single-cell transcriptomic data of the mouse brain [50], Nrf2 is relatively highly expressed in astrocytes but is barely expressed in neurons [51]. This is partially in accordance with our finding that celastrol reduces oxidative damage by regulating Nrf2 in astrocytes. Moreover, previous studies have shown that celastrol can activate Nrf2-related pathways [52,53]; however, the mechanism by which celastrol upregulates Nrf2 remains unknown. Our study uncovered that Nedd4, which promotes K48-linked ubiquitylation of Nrf2, is involved upstream of Nrf2 in astrocytes. Studies have reported that Nrf2 may undergo K48- or K63-linked ubiquitylation [54,55]. Generally, K48-linked ubiquitylation is related to protein degradation, whereas K63-linked ubiquitylation tends to regulate cell signaling [56]. We found that Nedd4, although capable of mediating K63-linked ubiquitination [41], drove Nrf2 degradation in astrocytes via K48-linked ubiquitylation, which was effectively blocked by celastrol. However, whether celastrol regulates Nrf2 by interacting with other molecules requires further investigation.

5. Conclusions

In summary, our data demonstrated that celastrol remarkably inhibited the accumulation of ROS after CIRI and showed great potential in therapies for patients with ischemic stroke. We found that celastrol attenuated oxidation by upregulating Nrf2 in astrocytes. Celastrol directly bound to Nedd4 and inhibited the interaction between Nedd4 and Nrf2, thus reducing the K48-linked ubiquitylation of Nrf2. We identified Nedd4 as an unrecognized E3 ligase of Nrf2 and elucidated a novel mechanism of celastrol's regulation of Nrf2. These findings provide convincing evidence that celastrol is a promising candidate in the search for a therapeutic strategy for ischemic stroke.

CRediT author statement

Zexuan Hong: Conceptualization, Formal analysis, Investigation, Methodology, Writing - Original draft preparation; **Jun Cao:** Conceptualization, Formal analysis, Investigation, Methodology, Writing - Original draft preparation; **Dandan Liu:** Conceptualization, Formal analysis, Investigation, Methodology; **Maozhu Liu**: Investigation; **Mengyuan Chen:** Investigation; **Fanning Zeng:** Investigation; **Zaisheng Qin:** Supervision, Funding acquisition, Project administration; **Jigang Wang:** Supervision, Funding acquisition, Writing - Reviewing and Editing; **Tao Tao:** Supervision, Funding acquisition, Project administration, Writing - Reviewing and Editing.

Declaration of competing interest

The authors declare that there are no conflicts of interest.

Acknowledgments

This work was funded by the National Natural Science Foundation of China (Grant No.: 81973305), the Science and Technology Planning Project of Guangzhou, China (Grant No.: 201904010487), the Natural Science Foundation of Guangdong Province, China (Grant No.: 2021A1515010897), and the Discipline Construction Fund of Central People's Hospital of Zhanjiang (Grant Nos.: 2020A01 and 2020A02). We also would like to thank Dr. Lei Li for her kind assistance in experiment implementation.

Appendix A. Supplementary data

Supplementary data to this article can be found online at https://doi.org/10.1016/j.jpha.2022.12.002.

References

[1] GBD 2019 Stroke Collaborators, Global, regional, and national burden of stroke and its risk factors, 1990–2019: A systematic analysis for the Global Burden of Disease Study 2019, Lancet Neurol. 20 (2021) 795–820.
[2] D. Kuriakose, Z. Xiao, Pathophysiology and treatment of stroke: Present status and future perspectives, Int. J. Mol. Sci. 21 (2020), 7609.
[3] M.-S. Sun, H. Jin, X. Sun, et al., Free radical damage in ischemia-reperfusion injury: An obstacle in acute ischemic stroke after revascularization therapy, Oxid. Med. Cell. Longev. 2018 (2018), 3804979.
[4] K. Lin, Z. Zhang, Z. Zhang, et al., Oleanolic acid alleviates cerebral ischemia/reperfusion injury via regulation of the gsk-3β/HO-1 signaling pathway, Pharmaceuticals (Basel) 15 (2021), 1.
[5] R. Dringen, Metabolism and functions of glutathione in brain, Prog. Neurobiol. 62 (2000) 649–671.
[6] R. Mao, N. Zong, Y. Hu, et al., Neuronal death mechanisms and therapeutic strategy in ischemic stroke, Neurosci. Bull. 38 (2022) 1229–1247.
[7] Y. Gürsoy-Ozdemir, A. Can, T. Dalkara, Reperfusion-induced oxidative/nitrative injury to neurovascular unit after focal cerebral ischemia, Stroke 35 (2004) 1449–1453.
[8] S. Xu, J. Lu, A. Shao, et al., Glial cells: Role of the immune response in ischemic stroke, Front. Immunol. 11 (2020), 294.
[9] H. Chen, H. Yoshioka, G.S. Kim, et al., Oxidative stress in ischemic brain damage: Mechanisms of cell death and potential molecular targets for neuroprotection, Antioxid. Redox Signal. 14 (2011) 1505–1517.
[10] P. Li, R.A. Stetler, R.K. Leak, et al., Oxidative stress and DNA damage after cerebral ischemia: Potential therapeutic targets to repair the genome and improve stroke recovery, Neuropharmacology 134 (2018) 208–217.
[11] R. He, Y. Jiang, Y. Shi, et al., Curcumin-laden exosomes target ischemic brain tissue and alleviate cerebral ischemia-reperfusion injury by inhibiting ROS-mediated mitochondrial apoptosis, Mater. Sci. Eng. C Mater. Biol. Appl. 117 (2020), 111314.
[12] H. Xu, J. Shen, J. Xiao, et al., Neuroprotective effect of cajaninstilbene acid against cerebral ischemia and reperfusion damages by activating AMPK/Nrf2 pathway, J. Adv. Res. 34 (2021) 199–210.
[13] S. Orellana-Urzúa, I. Rojas, L. Líbano, et al., Pathophysiology of ischemic stroke: Role of oxidative stress, Curr. Pharm. Des. 26 (2020) 4246–4260.
[14] R. Kannaiyan, M.K. Shanmugam, G. Sethi, Molecular targets of celastrol derived from Thunder of God Vine: Potential role in the treatment of inflammatory disorders and cancer, Cancer Lett. 303 (2011) 9–20.
[15] Y. Lu, Y. Liu, J. Zhou, et al., Biosynthesis, total synthesis, structural modifications, bioactivity, and mechanism of action of the quinone-methide triterpenoid celastrol, Med. Res. Rev. 41 (2021) 1022–1060.
[16] ClinicalTrials.gov, A sub-chronic evaluation of the safety of celastrol in human subjects. https://beta.clinicaltrials.gov/study/NCT05494112?distance=50&cond=celastrol&rank=2. (Accessed 25 September 2022).
[17] ClinicalTrials.gov, Effect of different ingestion doses of celastrol on human sperm motility. https://clinicaltrials.gov/ct2/show/NCT05413226?cond=celastrol&draw=2. (Accessed 25 September 2022).
[18] M. Li, X. Liu, Y. He, et al., Celastrol attenuates angiotensin II mediated human umbilical vein endothelial cells damage through activation of Nrf2/ERK1/2/Nox2 signal pathway, Eur. J. Pharmacol. 797 (2017) 124–133.
[19] A.C. Allison, R. Cacabelos, V.R. Lombardi, et al., Celastrol, a potent antioxidant and anti-inflammatory drug, as a possible treatment for Alzheimer's disease, Prog. Neuropsychopharmacol. Biol. Psychiatry 25 (2001) 1341–1357.
[20] B.S. Choi, H. Kim, H.J. Lee, et al., Celastrol from 'Thunder God Vine' protects SH-SY5Y cells through the preservation of mitochondrial function and inhibition of p38 MAPK in a rotenone model of Parkinson's disease, Neurochem. Res. 39 (2014) 84–96.
[21] C. Cleren, N.Y. Calingasan, J. Chen, et al., Celastrol protects against MPTP- and 3-nitropropionic acid-induced neurotoxicity, J. Neurochem. 94 (2005) 995–1004.
[22] M. Jiang, X. Liu, D. Zhang, et al., Celastrol treatment protects against acute ischemic stroke-induced brain injury by promoting an IL-33/ST2 axis-mediated microglia/macrophage M2 polarization, J. Neuroinflammation 15 (2018), 78.
[23] D.-D. Liu, P. Luo, L. Gu, et al., Celastrol exerts a neuroprotective effect by directly binding to HMGB1 protein in cerebral ischemia-reperfusion, J. Neuroinflammation 18 (2021), 174.
[24] J. Cao, L. Dong, J. Luo, et al., Supplemental N-3 polyunsaturated fatty acids limit A1-specific astrocyte polarization via attenuating mitochondrial dysfunction in ischemic stroke in mice, Oxid. Med. Cell. Longev. 2021 (2021), 5524705.
[25] R. Verma, C.G. Cronin, J. Hudobenko, et al., Deletion of the P2X4 receptor is neuroprotective acutely, but induces a depressive phenotype during recovery from ischemic stroke, Brain Behav. Immun. 66 (2017) 302–312.
[26] D. Liu, M. Zhang, X. Rong, et al., Potassium 2-(1-hydroxypentyl)-benzoate attenuates neuronal apoptosis in neuron-astrocyte co-culture system through neurotrophy and neuroinflammation pathway, Acta Pharm. Sin. B 7 (2017) 554–563.
[27] B. Zhou, Y.-X. Zuo, R.-T. Jiang, Astrocyte morphology: Diversity, plasticity, and role in neurological diseases, CNS Neurosci. Ther. 25 (2019) 665–673.
[28] M.V. Sofroniew, Astrocyte reactivity: Subtypes, states, and functions in CNS innate immunity, Trends Immunol. 41 (2020) 758–770.
[29] S. Jiang, C. Deng, J. Lv, et al., Nrf2 weaves an elaborate network of neuroprotection against stroke, Mol. Neurobiol. 54 (2017) 1440–1455.
[30] T.W. Kensler, N. Wakabayashi, S. Biswal, Cell survival responses to environmental stresses via the Keap1-Nrf2-ARE pathway, Annu. Rev. Pharmacol. Toxicol. 47 (2007) 89–116.
[31] J. Gao, Y. Zhang, X. Liu, et al., Triptolide: Pharmacological spectrum, biosynthesis, chemical synthesis and derivatives, Theranostics 11 (2021) 7199–7221.
[32] J. Li, J. Hao, Treatment of neurodegenerative diseases with bioactive components of *Tripterygium wilfordii*, Am. J. Chin. Med. 47 (2019) 769–785.
[33] T.W. Corson, C.M. Crews, Molecular understanding and modern application of traditional medicines: Triumphs and trials, Cell 130 (2007) 769–774.
[34] M. De Angelis, S.C. Schriever, E. Kyriakou, et al., Detection and quantification of the anti-obesity drug celastrol in murine liver and brain, Neurochem. Int. 136 (2020), 104713.
[35] M. Chen, M. Liu, Y. Luo, et al., Celastrol protects against cerebral ischemia/reperfusion injury in mice by inhibiting glycolysis through targeting HIF-1α/PDK1 axis, Oxid. Med. Cell. Longev. 2022 (2022), 7420507.
[36] C. Wang, H. Wan, M. Li, et al., Celastrol attenuates ischemia/reperfusion-mediated memory dysfunction by downregulating AK005401/MAP3K12, Phytomedicine 82 (2021), 153441.
[37] Z. Liu, M. Chopp, Astrocytes, therapeutic targets for neuroprotection and neurorestoration in ischemic stroke, Prog. Neurobiol. 144 (2016) 103–120.
[38] I. Lopez-Fabuel, J. Le Douce, A. Logan, et al., Complex I assembly into supercomplexes determines differential mitochondrial ROS production in neurons and astrocytes, Proc. Natl. Acad. Sci. U S A 113 (2016) 13063–13068.
[39] N.A. Boase, S. Kumar, NEDD4: The founding member of a family of ubiquitin-protein ligases, Gene 557 (2015) 113–122.
[40] S. Kumar, K.F. Harvey, M. Kinoshita, et al., cDNA cloning, expression analysis, and mapping of the mouse *Nedd4* gene, Genomics 40 (1997) 435–443.
[41] X. Ding, J. Jo, C.Y. Wang, et al., The Daam2-VHL-Nedd4 axis governs developmental and regenerative oligodendrocyte differentiation, Genes Dev. 34 (2020) 1177–1189.
[42] H.E. Hsia, R. Kumar, R. Luca, et al., Ubiquitin E3 ligase Nedd4-1 acts as a downstream target of PI3K/PTEN-mTORC1 signaling to promote neurite growth, Proc. Natl. Acad. Sci. U S A 111 (2014) 13205–13210.
[43] J. Drinjakovic, H. Jung, D.S. Campbell, et al., E3 ligase Nedd4 promotes axon branching by downregulating PTEN, Neuron 65 (2010) 341–357.
[44] Y.D. Kwak, B. Wang, J.J. Li, et al., Upregulation of the E3 ligase NEDD4-1 by oxidative stress degrades IGF-1 receptor protein in neurodegeneration, J. Neurosci. 32 (2012) 10971–10981.
[45] J. Lackovic, J. Howitt, J.K. Callaway, et al., Differential regulation of Nedd4 ubiquitin ligases and their adaptor protein Ndfip1 in a rat model of ischemic stroke, Exp. Neurol. 235 (2012) 326–335.
[46] S. Haouari, P. Vourc'h, M. Jeanne, et al., The roles of NEDD4 subfamily of HECT E3 ubiquitin ligases in neurodevelopment and neurodegeneration, Int. J. Mol. Sci. 23 (2022), 3882.
[47] L. Gao, H.-J. Wang, C. Tian, et al., Skeletal muscle Nrf2 contributes to exercise-evoked systemic antioxidant defense via extracellular vesicular communication, Exerc. Sport Sci. Rev. 49 (2021) 213–222.
[48] B.J. Saeedi, K.H. Liu, J.A. Owens, et al., Gut-resident *Lactobacilli* activate hepatic Nrf2 and protect against oxidative liver injury, Cell Metab. 31 (2020) 956–968.
[49] L. Kong, J. Deng, X. Zhou, et al., Sitagliptin activates the p62-Keap1-Nrf2 signalling pathway to alleviate oxidative stress and excessive autophagy in severe acute pancreatitis-related acute lung injury, Cell Death Dis. 12 (2021), 928.
[50] A. Saunders, E.Z. Macosko, A. Wysoker, et al., Molecular diversity and specializations among the cells of the adult mouse brain, Cell 174 (2018) 1015–1030.e16.
[51] S.M. Boas, K.L. Joyce, R.M. Cowell, The NRF2-dependent transcriptional regulation of antioxidant defense pathways: Relevance for cell type-specific vulnerability to neurodegeneration and therapeutic intervention, Antioxidants (Basel) 11 (2021), 8.
[52] T. Nakayama, K. Okimura, J. Shen, et al., Seasonal changes in NRF2 antioxidant pathway regulates winter depression-like behavior, Proc. Natl. Acad. Sci. U S A 117 (2020) 9594–9603.
[53] C. Zhang, M. Zhao, B. Wang, et al., The Nrf2-NLRP3-caspase-1 axis mediates the neuroprotective effects of Celastrol in Parkinson's disease, Redox Biol. 47 (2021), 102134.
[54] W. Gong, Z. Chen, Y. Zou, et al., CKIP-1 affects the polyubiquitination of Nrf2 and Keap1 via mediating Smurf1 to resist HG-induced renal fibrosis in GMCs and diabetic mice kidneys, Free Radic. Biol. Med. 115 (2018) 338–350.
[55] D.J. McIntosh, T.S. Walters, I.J. Arinze, et al., Arkadia (RING finger protein 111) mediates sumoylation-dependent stabilization of Nrf2 through K48-linked ubiquitination, Cell. Physiol. Biochem. 46 (2018) 418–430.
[56] K. Hochrainer, Protein modifications with ubiquitin as response to cerebral ischemia-reperfusion injury, Transl. Stroke Res. 9 (2018) 157–173.